Rock Mech Rock Eng (2017) 50:2177–2192
DOI 10.1007/s00603-017-1210-6

ORIGINAL PAPER

Prediction of Fragmentation Zone Induced by Blasting in Rock

Youngjong Sim[1] · Gye-Chun Cho[2] · Ki-Il Song[3]

Received: 14 July 2016 / Accepted: 24 March 2017 / Published online: 10 April 2017

Abstract This paper presents a simple method to evaluate the two-dimensional fragmentation zone induced by gas pressure during blasting in rock. The fragmentation zone is characterized by analyzing crack propagation from the blasthole. To do this, a model of the blasthole with a number of radial cracks of equal length in an infinite elastic plane is considered. In this model, the crack propagation is simulated by using two conditions only, the crack propagation criterion and the mass conservation of the gas. As a result, the stress intensity factor of the crack decreases as crack propagates from the blasthole so that the crack length is determined. In addition, gas pressure inside blasthole also continues to decrease during crack propagation. To validate suggested analytical solution, discrete element method is used by comparing length of propagated crack due to blasting.

Keywords Blasting · Crack propagation · Fragmentation zone · Gas pressure · Stress intensity factor

✉ Ki-Il Song
ksong@inha.ac.kr

Youngjong Sim
yjsim@lh.or.kr

Gye-Chun Cho
gyechun@kaist.edu

[1] Land and Housing Institute, Korea Land and Housing Corporation (LH), 539-99 Expo-ro, Yuseong-gu, Daejeon 34047, Korea

[2] Department of Civil and Environmental Engineering, Korea Advanced Institute of Science and Technology (KAIST), Daejeon 34141, Korea

[3] Department of Civil Engineering, Inha University, 100 Inha-ro, Nam-gu, Incheon 22212, Korea

List of symbols

γ	Adiabatic exponent
ΔM	Mass change of gas (kg)
ΔV	Change of volume (m^3/m)
$\Delta V_{\text{blasthole}}$	Change of blasthole volume (m^3/m)
ν	Poisson's ratio
ρ	Density of explosive (kg/m^3)
ρ_{g}	Density of the gas (kg/m^3)
ρ_{gi}	Density of the gas at the moment of crack initiation (kg/m^3)
E	Elastic modulus of the rock (Pa)
f_{Z}	Summation of dimensionless functions of crack volume and blasthole volume in problem Z (A, B) $(=f_{\text{Z}}^{\text{crack}}+f_{\text{Z}}^{\text{blasthole}})$
$f_{\text{Z}}^{\text{blasthole}}$	Dimensionless function of blasthole volume in problem Z (A, B)
$f_{\text{Z}}^{\text{crack}}$	Dimensionless function of crack volume in problem Z (A, B)
K_{I}	Stress intensity factor for mode I (Pa $m^{1/2}$)
K_{Ic}	Fracture toughness for mode I in rock (Pa $m^{1/2}$)
K_{IZ}	Stress intensity factor for mode I in problem Z (A, B) (Pa $m^{1/2}$)
$k_{\text{IZ}}^{\text{crack}}$	Dimensionless function of stress intensity factor for mode I in problem Z (A, B)
l	Length of crack propagation (m)
$M_{\text{blasthole}}$	Mass of gas in the blasthole (kg)
M_{crack}	Mass of gas in the crack (kg)
M_{i}	Mass of gas in the blasthole at the moment of crack initiation (kg)
N	Number of cracks
p_0	Gas pressure (Pa)
p_{A}	Gas pressure applied to the blasthole (Pa)
p_{B}	Gas pressure applied to the crack (Pa)

p_i	Gas pressure at the moment of crack initiation (Pa)
P_B	Maximum blasthole pressure (Pa)
r	Blasthole radius (m)
r_c	Decoupling ratio (i.e., explosive diameter/bore hole diameter)
V	Total deformed volume of blasthole and crack (m^3/m)
$V_{blasthole}$	Deformed volume of the blasthole by gas pressure (m^3/m)
V_{crack}	Deformed volume of the crack by gas pressure (m^3/m)
$V_Z^{blasthole}$	Deformed volume of blasthole in problem Z (A, B) (m^3/m)
V_Z^{crack}	Deformed volume of crack in problem Z (A, B) (m^3/m)
V_i	Deformed volume of the blasthole by gas pressure at the moment of crack initiation (m^3/m)
VOD	Velocity of detonation (m/s)

1 Introduction

It is of great importance to evaluate a blasting-induced fragmentation zone beyond the proposed excavation line of a tunnel because the unwanted damaged zone requires extra support systems for tunnel safety. However, complicated blasting process which may hinder a proper characterization of the damaged zone can be effectively represented by two loading mechanisms (e.g., Brinkman 1987). The first one is a dynamic impulsive load generating stress waves that radiate outwards immediately after detonation. This load creates a crushed annulus around blasthole with many radial cracks (fracture zone in Fig. 1) and remains in the order of micro-seconds. The second one is a gas pressure that remains for a few micro-seconds, which is relatively long time. Since the gas pressure reopens up the arrested cracks and continues to extend some cracks, it contributes to the formation of fragmentation zone (Fig. 1) induced by blasting.

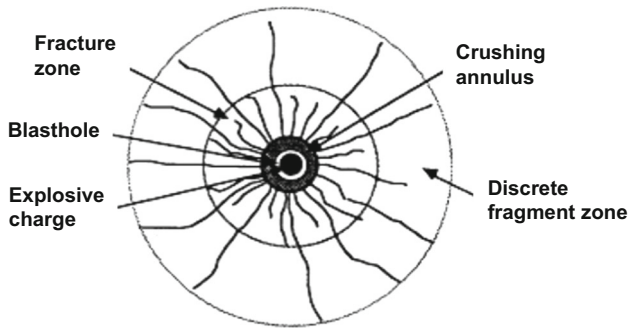

Fig. 1 Fracture process of explosive blasting (Whittaker et al. 1992)

Although Fjellborg and Olsson (1996), Olsson et al. (2004), Mindess (1991), Rossmanith (1983) and Maji and Wang (1992) carried out experimental test to predict the blasting-induced crack propagation, they do not explain the mechanisms involved with the fragmentation process.

Recent advances in the numerical simulation tools which have powerful computational functions have made numerical analysis a most promising approach to study the fracturing processes in rock mass. Particularly, to simulate the crack propagation due to blasting, various numerical methods have been used. Zhu et al. (2007a, b), Chen and Zhao (1998) and Ma et al. (1998) conducted numerical study with AUTODYN code for simulation of rock fracturing. AUTODYN code has been applied to solve nonlinear problems based on the Lagrange computation scheme. This code can be used to simulate the rock fragmentation due to blasting. To consider the gas flow through the crack, finite difference method (FDM), which uses Lagrangian computation process, also has been adopted by Cho et al. (2004b), Goodarzi et al. (2011, 2013), and Cho et al. (2002).

A finite element method (FEM) such as ABAQUS has been used to simulate a brittle cracking in brittle rock (Saharan and Mitri 2008). However, explicit crack generation cannot be effectively presented with general FEM code. To overcome this limitation, XFEM has been used to simulate the crack propagation in solid media. Fracturing of rock mass is also studied with the powerful extended finite element method (XFEM) (Majid et al. 2015; Ren et al. 2009). Recently, advanced XFEM which can consider hydro-mechanical coupling has been introduced in various researches (Mohammadnejad and Khoei 2013; Gordeliy and Peirce 2013; Gholami et al. 2013).

To simulate the rock fragmentation, various numerical methods have been used: three-dimensional discrete element program PFC3D (Potyondy et al. 2004), combined finite element–discrete element program MBM2D (Minchinton and Lynch 1996), cross-format centered finite difference procedure (Wang et al. 2008), AUTODYN 2D (Zhu et al. 2007a, b), Johnson–Holmquist model in LS-DYNA (Ma and An 2008), ANSYS–LSDYNA (Wei et al. 2009), fully coupled gas flow-lattice model (Onederra et al. 2013), DEM–SPH simulation (Ali and Mark 2014). A summary of numerical analysis on crack propagation due to blasting is presented by Ali and Mark (2014).

Ouchterlony (1997), Ouchterlony et al. (2002) gave an equation for estimating radial crack length. Hustrulid (2010) analyzed the energy and work done by an explosive charge in a borehole to develop the extent of damage based on explosive energy. Kanchibolta et al. (1999) offered an equation to estimate the crushing zone radius. Although

these works tried to provide theoretical solution for the blasting-induced damaged zone, simplification and assumption cannot be avoided due to the complexity involved with the fragmentation process. And these models are only considered for estimating the extent of the blast-damaged zone (Torbica and Lapcevic 2015). In fact, there are several studies to evaluate fragmentation zone by introducing gas-driven fractures in blasting (e.g., Nilson et al. 1985; Paine and Please 1994). To study the gas fracturing process, the deformation of the rock around blasthole and gas flow needs to be considered (Paine and Please 1994).

In this paper, the simple analytical method is presented to evaluate the fragmentation zone induced by gas pressure during blasting in rock. The fragmentation zone is characterized by analyzing crack propagation from the blasthole.

2 Evaluation of Crack Propagation from the Blasthole

2.1 Basic Assumptions

To evaluate crack propagation in rock, a model of blasthole with radial cracks is introduced in an infinite elastic plane (Fig. 2). Two-dimensional plane is applied since the diameter of blasthole is far smaller than its length and there is no free surface.

The typical number of symmetric cracks of equal length around blasthole is chosen in an elastic rock and is assumed to propagate radially from the blasthole by gas pressure. It was experimentally investigated that the number of main cracks that could be formed ranges from 3 to 8 (Garnsworthy 1990) even though a huge number of cracks would be generated after detonation. For the simplicity, the number of major cracks for model is assumed to be four ($N = 4$) and eight ($N = 8$), which are symmetric.

In Fig. 2, the gas pressure is applied to the blasthole and is penetrated into the cracks. p_A and p_B are gas pressures applied to the blasthole and cracks, respectively. It is assumed that the distribution of pressure along blasthole is uniform. In the case of pressure inside cracks, two types of pressure distribution, uniform and linear pressure distributions, are considered for the analysis. Uniform pressure distribution gives upper bound estimation of calculating crack length (Fig. 2a). Due to the fast crack propagation during blasting and narrow opening of the crack, however, the actual pressure inside cracks will not be distributed uniformly so that linear pressure distribution is also considered for the analysis. In case of linear pressure distribution, p_B is the pressure at the crack mouth (Fig. 2b).

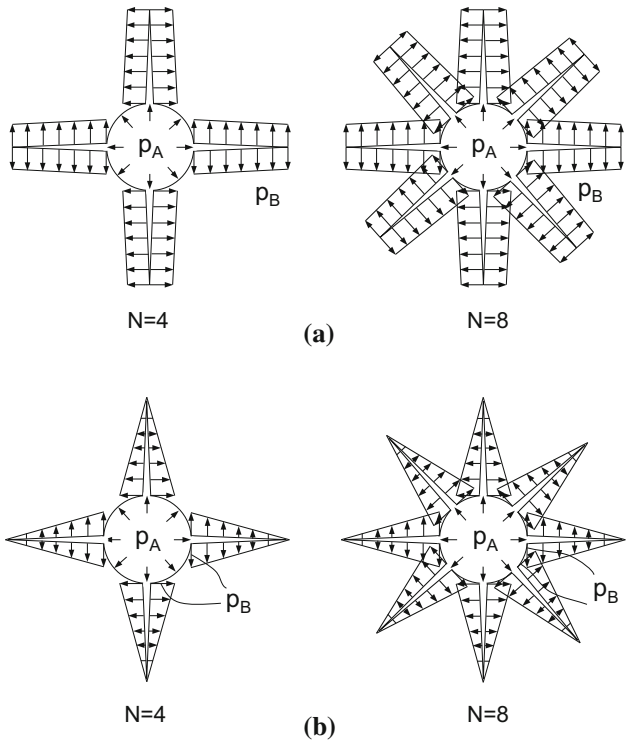

Fig. 2 Pressurized blasthole and propagating radial cracks. **a** Uniform pressure inside blasthole and cracks, and **b** uniform pressure inside blasthole and linear pressure inside cracks

Simply, two conditions only are considered to describe the crack propagation in this paper. The first condition is the criterion for crack propagation. It states that the stress intensity factor (SIF) for mode I, K_I, needs to be greater than the fracture toughness K_{IC}, that is, $K_I > K_{IC}$. The second condition indicates that the total mass of gas in the blasthole and cracks need to be conserved. That is, the mass change, ΔM, needs to be equal to zero. Based on these two conditions, the final fragmented area is characterized by analyzing the probable length of the crack propagation at given conditions. It may be reasonable to ignore the effect of gravity because the explosive pressure is expected to highly exceed the in situ stress.

2.2 Formulation

The total mass of gas during the crack propagation remains constant as following:

$$M_{\text{blasthole}} + M_{\text{crack}} = M_i \tag{1}$$

where $M_{\text{blasthole}}$ and M_{crack} are the mass of gas in the blasthole and the crack, respectively. And M_i is the mass of gas in the blasthole at the moment of crack initiation when

most of the gas is assumed to be generated. Each mass of the gas in Eq. (1) can be expressed as follows:

$$M_{\mathrm{i}} = V_{\mathrm{i}}\rho_{\mathrm{gi}} \tag{2}$$

$$M_{\mathrm{blasthole}} = V_{\mathrm{blasthole}}\rho_{\mathrm{g}} \tag{3}$$

$$M_{\mathrm{crack}} = V_{\mathrm{crack}}\rho_{\mathrm{g}} \tag{4}$$

where V_{i}, $V_{\mathrm{blasthole}}$, and V_{crack} are volume of the blasthole at the moment of crack initiation, volume of the blasthole, and volume of the crack by gas pressure, respectively. The density of the gas, ρ_{g}, during the blasting follows adiabatic process. Then

$$\rho_{\mathrm{g}} = \left(\frac{p}{p_{\mathrm{i}}}\right)^{\frac{1}{\gamma}} \cdot \rho_{\mathrm{gi}} \tag{5}$$

where γ is the adiabatic exponent ranging from 1.2 to 3 in blasting (e.g., Paine and Please 1994; Persson et al. 1994), ρ_{gi} and p_{i} are the density of the gas and pressure at the moment of crack initiation, respectively. p_{i} is reasonably assumed to be peak pressure since the most of the gas is generated at the moment of crack initiation.

It is assumed that the uniform pressure inside cracks is same as that of blasthole as follows:

$$p_{\mathrm{A}} = p_{\mathrm{B}} = p_0 \tag{6}$$

In case of linear pressure distribution, above Eq. (6) is valid since the pressure at the crack mouth, p_{B}, is also same as pressure in blasthole, p_{A}. Substituting Eqs. (2)–(6) into Eq. (1), we obtain

$$V_{\mathrm{blasthole}}\left(\frac{p_0}{p_{\mathrm{i}}}\right)^{\frac{1}{\gamma}} + V_{\mathrm{crack}}\left(\frac{p_0}{p_{\mathrm{i}}}\right)^{\frac{1}{\gamma}} = V_{\mathrm{i}} \tag{7}$$

As shown in Eq. (7), volumes of the blasthole and cracks in proposed model (Fig. 2) need to be evaluated for arbitrary gas pressure. To simply do this, an original model is decomposed into two auxiliary problems as shown in Fig. 3. In Problem A, the gas pressure is applied only inside blasthole but no pressure inside cracks. In Problem B, the gas pressure is applied only inside cracks but no pressure inside blasthole. Each problem is affected by one single parameter, p_0.

In both problems, the SIFs of the cracks and volumes of the cracks and blasthole can be expressed as

$$K_{\mathrm{IZ}} = p_0\sqrt{\pi r}\,k_{\mathrm{IZ}}^{\mathrm{crack}}(l, r) \tag{8}$$

$$V_{\mathrm{Z}}^{\mathrm{crack}} = \frac{p_0 r^2}{E} f_{\mathrm{Z}}^{\mathrm{crack}}(v, l, r) \tag{9}$$

$$V_{\mathrm{Z}}^{\mathrm{blasthole}} = \frac{p_0 r^2}{E} f_{\mathrm{Z}}^{\mathrm{blasthole}}(v, l, r) \tag{10}$$

where subscript Z is A or B, K_{IZ} is SIF of the crack in problem Z, $V_{\mathrm{Z}}^{\mathrm{crack}}$ and $V_{\mathrm{Z}}^{\mathrm{blasthole}}$ are volumes of cracks and blasthole in problem Z, respectively, $k_{\mathrm{IZ}}^{\mathrm{crack}}$, $f_{\mathrm{Z}}^{\mathrm{crack}}$, and $f_{\mathrm{Z}}^{\mathrm{blasthole}}$ are dimensionless functions to be determined in plane strain condition using finite element code, FRANC2D (Wawrzynek and Ingraffea 1987), l and r are the crack propagation length and blasthole radius, respectively, and v and E are Poisson's ratio and elastic modulus of the rock, respectively. Also, $k_{\mathrm{IZ}}^{\mathrm{crack}}$ is the function of l and r, and both $f_{\mathrm{Z}}^{\mathrm{crack}}$ and $f_{\mathrm{Z}}^{\mathrm{blasthole}}$ are functions of v, l, and r.

Suppose that all three dimensionless functions with respect to the radial crack length, l, are known from the numerical calculations (refer to "Appendix"). Then, the superposition of problems A and B results in

$$K_{\mathrm{I}} = \left(p_0 k_{\mathrm{IA}}^{\mathrm{crack}}(l, r) + p_0 k_{\mathrm{IB}}^{\mathrm{crack}}(l, r)\right)\sqrt{\pi r} \tag{11}$$

$$V_{\mathrm{crack}} = \frac{p_0 c^2}{E} f_{\mathrm{A}}^{\mathrm{crack}}(v, l, r) + \frac{p_0 c^2}{E} f_{\mathrm{B}}^{\mathrm{crack}}(v, l, r) \tag{12}$$

$$V_{\mathrm{blasthole}} = \frac{p_0 c^2}{E} f_{\mathrm{A}}^{\mathrm{blasthole}}(v, l, r) + \frac{p_0 c^2}{E} f_{\mathrm{B}}^{\mathrm{blasthole}}(v, l, r) \tag{13}$$

Our notations can be further simplified by introducing the function

$$f_{\mathrm{Z}} = f_{\mathrm{Z}}^{\mathrm{crack}}(v, l, r) + f_{\mathrm{Z}}^{\mathrm{blasthole}}(v, l, r) \tag{14}$$

And the total volume can be

$$V = V_{\mathrm{crack}} + V_{\mathrm{blasthole}} = \frac{p_0 r^2}{E} f_{\mathrm{A}}(v, l, r) + \frac{p_0 r^2}{E} f_{\mathrm{B}}(v, l, r) \tag{15}$$

To calculate the change of the total volume due to crack propagation, the initial volume of the pressurized blasthole should be subtracted and can be expressed as:

$$V_{\mathrm{i}} = \frac{p_{\mathrm{i}} r^2}{E} f_{\mathrm{A}}(v, l = 0, r) \tag{16}$$

In above Eq. (16), it is assumed that the crack length is zero ($l = 0$) at the moment of initiation. Then, the total volume change due to crack propagation is obtained by subtracting Eq. (16) from Eq. (15):

$$\Delta V = \frac{p_0 r^2}{E} f_{\mathrm{A}}(v, l, r) + \frac{p_0 r^2}{E} f_{\mathrm{B}}(v, l, r) - \frac{p_{\mathrm{i}} r^2}{E} f_{\mathrm{A}}(v, 0, r) \tag{17}$$

The change of blasthole volume, meanwhile, is defined as

$$\Delta V_{\mathrm{blasthole}} = V_{\mathrm{blasthole}} - V_{\mathrm{i}} \tag{18}$$

Inserting Eq. (18) into Eq. (7) yields

$$\Delta V_{\mathrm{blasthole}} + V_{\mathrm{crack}} = \Delta V = V_{\mathrm{i}}\left\{\left(\frac{p_{\mathrm{i}}}{p_0}\right)^{\frac{1}{\gamma}} - 1\right\} \tag{19}$$

From Eqs. (17) and (19)

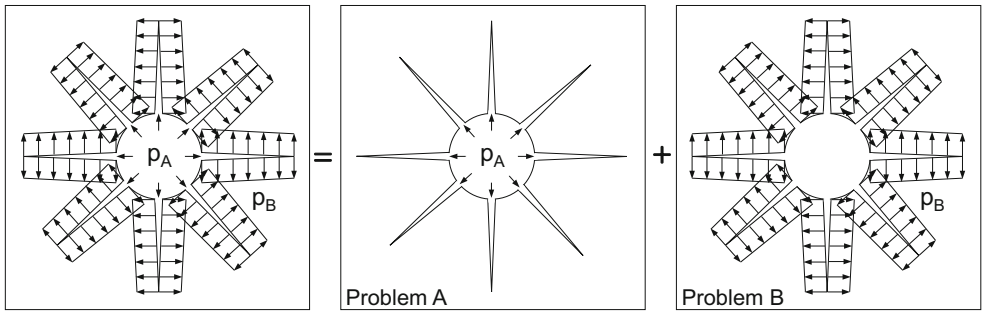

(a)

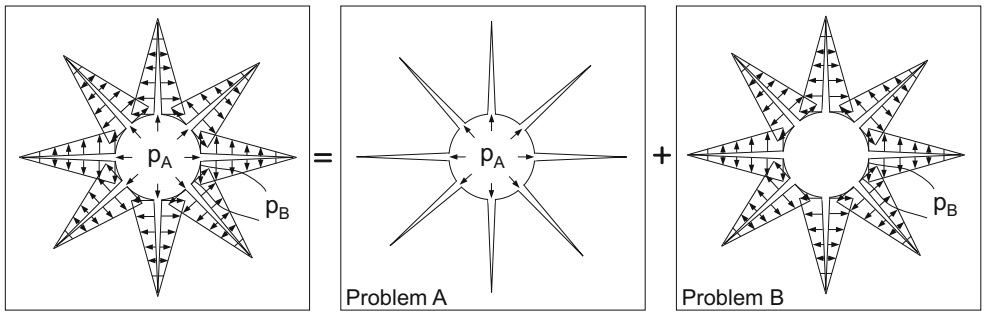

(b)

Fig. 3 Decomposition of the original model ($N = 8$, uniform pressure) into two sub-problems. **a** Uniform pressure model and **b** linear pressure model

$$p_0 f_A(v,l,r) + p_0 f_B(v,l,r) - p_i f_A(v,0,r) = f_A(v,0,r) p_i \left\{ \left(\frac{p_0}{p_i} \right)^{\frac{1}{\gamma}} - 1 \right\} \quad (20)$$

Finally, gas pressure can be derived as follows:

$$p_0 = p_i \left(\frac{f_A(v,0,r)}{f_A(v,l,r) + f_B(v,l,r)} \right)^{\frac{\gamma}{\gamma+1}} \quad (21)$$

In addition, following condition should be satisfied for the crack propagation.

$$K_I \geq K_{Ic} \quad (22)$$

Therefore, using Eq. (11), finally propagated length of the crack can be determined from the following equation.

$$K_I = (p_0 k_{IA}(l,r) + p_0 k_{IB}(l,r)) \sqrt{\pi r} \geq K_{Ic} \quad (23)$$

2.3 No Gas Penetration into the Crack

Ouchterlony (1974) illustrated various pressure distribution conditions including no gas penetration into the cracks in relation to rock blasting. During the blasting, crushing annulus created by stress wave may prevent gas penetration into the cracks so that it is closely related to the blasting efficiency. To deal with this condition, only Problem A out of two auxiliary problems can be considered. Iterating same formulation procedure, equations for gas pressure and SIF can be obtained as follows:

$$p_0 = p_i \left(\frac{f_A(v,0,r)}{f_A(v,l,r)} \right)^{\frac{\gamma}{\gamma+1}} \quad (24)$$

$$K_I = p_0 k_{IA}(l,r) \sqrt{\pi r} \geq K_{Ic} \quad (25)$$

Therefore, it is expected that the crack length obtained from Eq. (25) gives lower estimate while one from Eq. (23) gives upper estimate.

3 Results and Discussion

Two cases that have distinctly different elastic properties of the rocks for the analyses are shown in Table 1. Case 1 corresponds to the hard rock property while Case 2 corresponds to the weathered rock property. For the comparison, the same initial gas pressure, p_i, is applied. The

Table 1 Two different elastic properties of the rocks and initial gas pressure for the analyses

Properties	E (Pa)	v	K_{Ic} (Pa m$^{1/2}$)	p_i (MPa)
Case 1	21E9	0.2	2.5E6	100
Case 2	2E9	0.28	0.5E6	100

diameter of blasthole, $2r$, and the adiabatic exponent, γ, are fixed as 0.045 m and 3, respectively.

Figures 4 and 5 show the comparison of the normalized SIFs and gas pressure variations in blasthole between Case 1 and Case 2 for both uniform and linear pressure distribution inside crack. The normalized SIFs generally decrease as cracks propagate. However, the crack can only propagate if the normalized SIF (K_I/K_{Ic}) is greater than

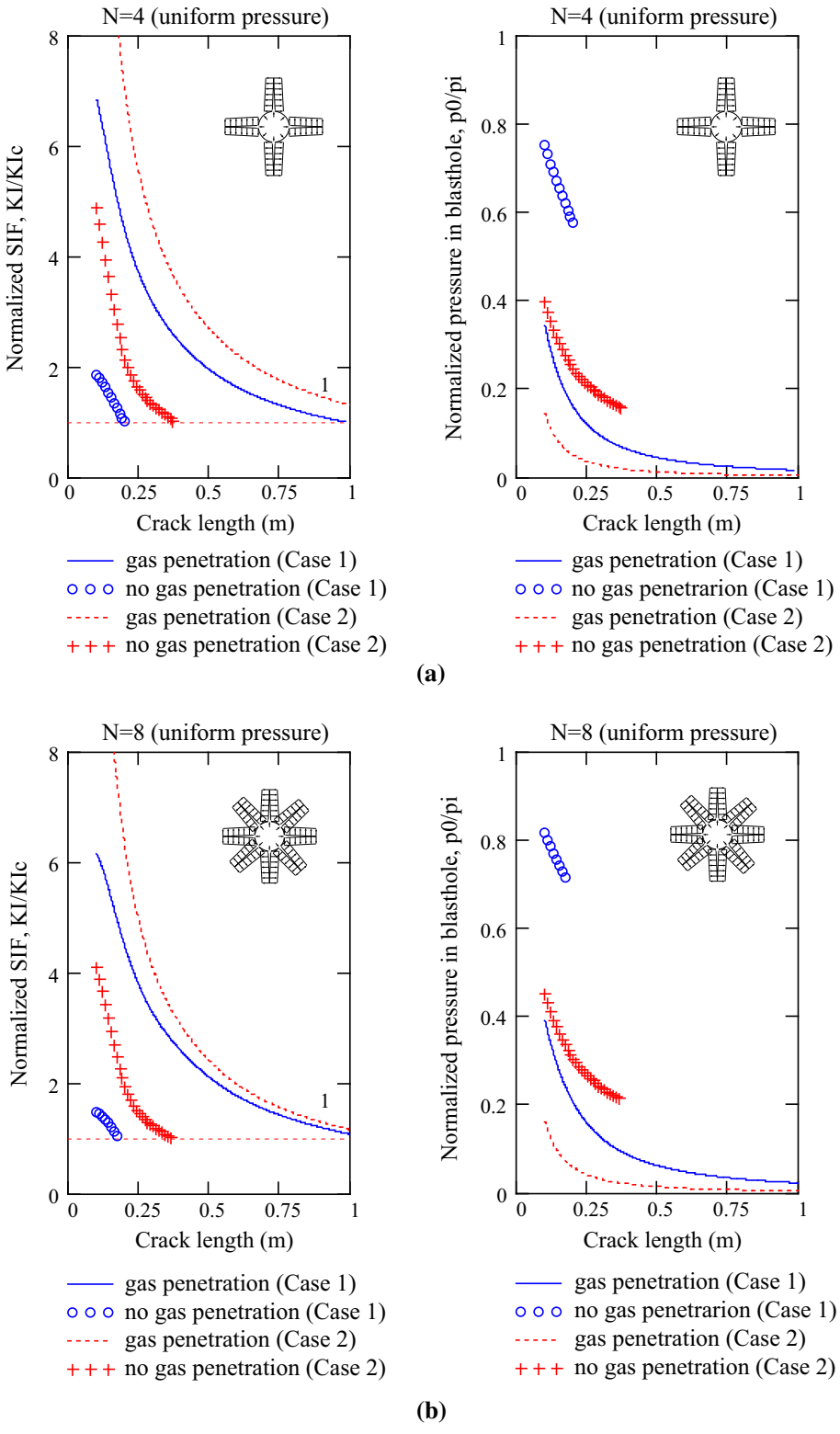

Fig. 4 Comparison of the SIFs and gas pressure between Case 1 and Case 2 for uniform pressure distribution inside cracks. **a** $N = 4$, and **b** $N = 8$

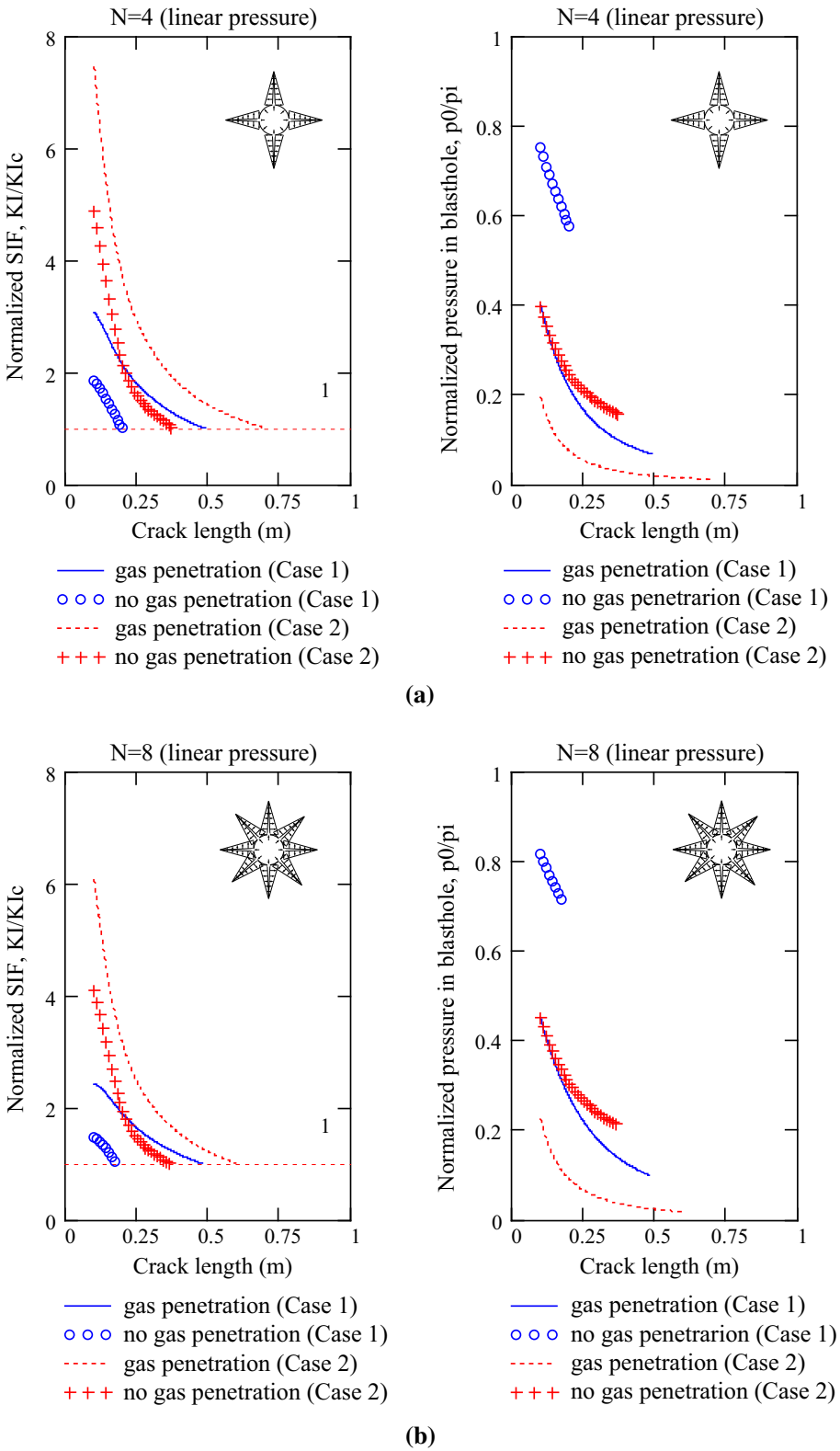

Fig. 5 Comparison of the SIFs and gas pressure between Case 1 and Case 2 for linear pressure distribution inside cracks. **a** $N = 4$, and **b** $N = 8$

one. As expected, longer crack is obtained in Case 2 than in Case 1. For example, in case of Case 2 and uniform pressure inside crack as in Fig. 4a, obtained crack length is larger than 1 m, while in case of Case 1 with same pressure condition, obtained crack length is about to 0.98 m. Also, if the gas does not penetrate into the cracks, the obtained

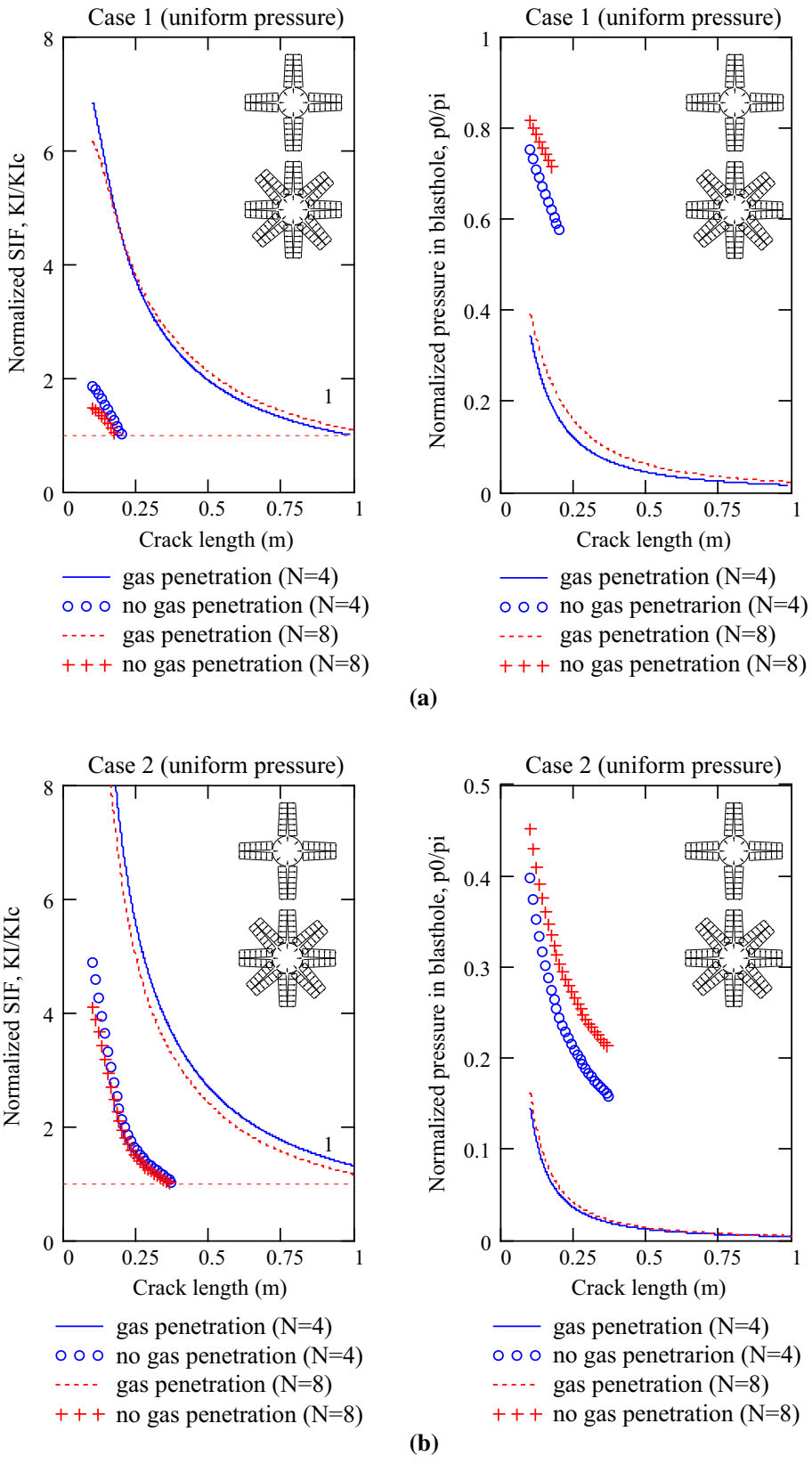

Fig. 6 Comparison of the SIFs and gas pressure between $N = 4$ and $N = 8$ cases for uniform pressure distribution inside cracks. **a** Case 1, and **b** Case 2

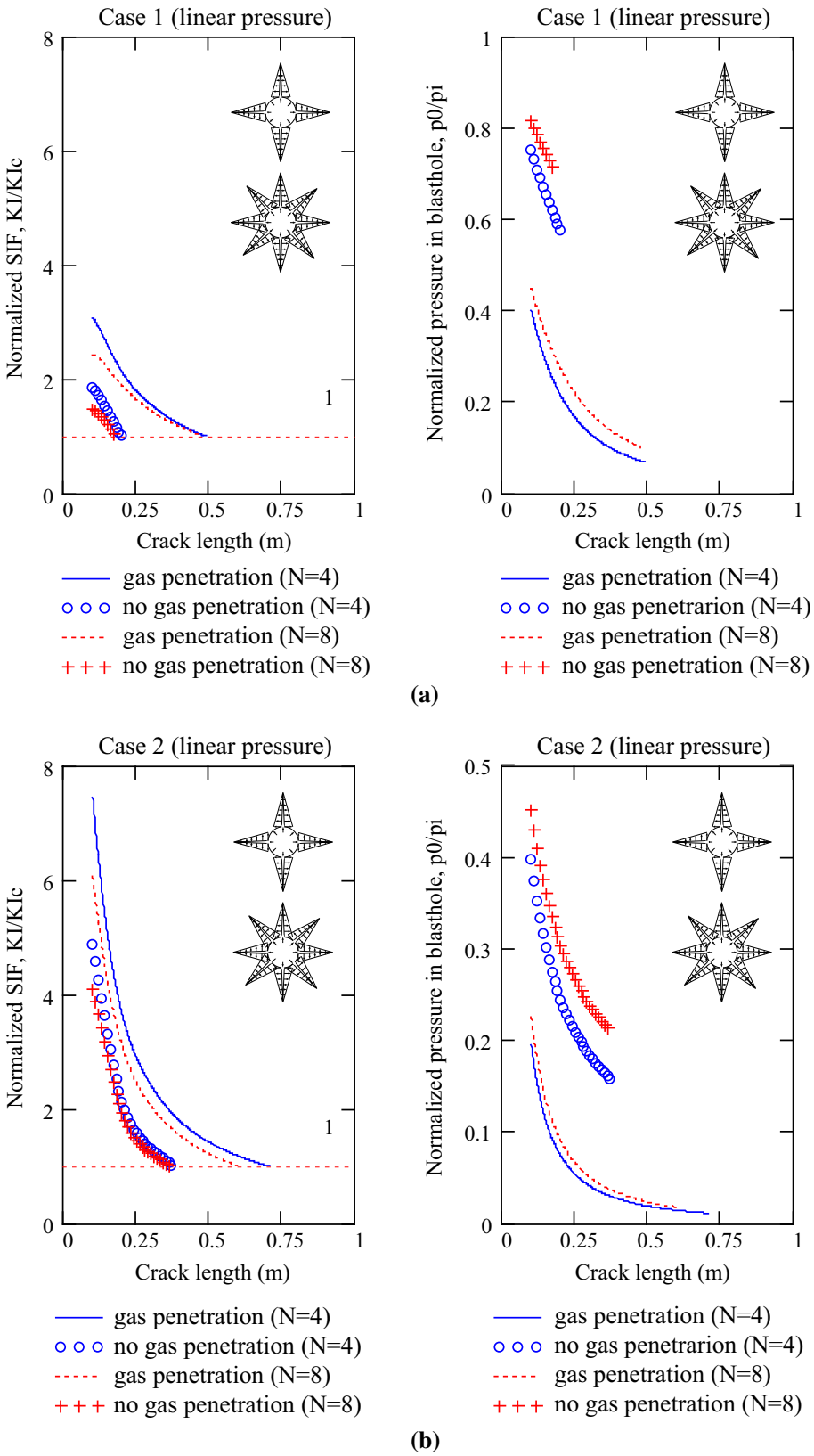

Fig. 7 Comparison of the SIFs and gas pressure between $N = 4$ and $N = 8$ cases for linear pressure distribution inside cracks. **a** Case 1, and **b** Case 2

Table 2 Summary of finally propagated lengths of the cracks (unit: m)

	$N = 4$		$N = 8$	
	Case 1	Case 2	Case 1	Case 2
Pressure type ($p_i = 50$ MPa)				
Uniform pressure	0.49	0.66	0.53	0.59
Linear pressure	0.22	0.36	0.18	0.31
No gas penetration	–	0.21	–	0.20
Pressure type ($p_i = 100$ MPa)				
Uniform pressure	0.98	1.30	1.07	1.15
Linear pressure	0.49	0.71	0.48	0.60
No gas penetration	0.20	0.38	0.18	0.36
Pressure type ($p_i = 150$ MPa)				
Uniform pressure	1.47	1.95	1.61	1.69
Linear pressure	0.75	1.05	0.75	0.9
No gas penetration	0.30	0.52	0.26	0.51
Pressure type ($p_i = 200$ MPa)				
Uniform pressure	1.98	–	2.23	2.28
Linear pressure	1.01	1.40	1.03	1.20
No gas penetration	0.40	0.67	0.01	0.67

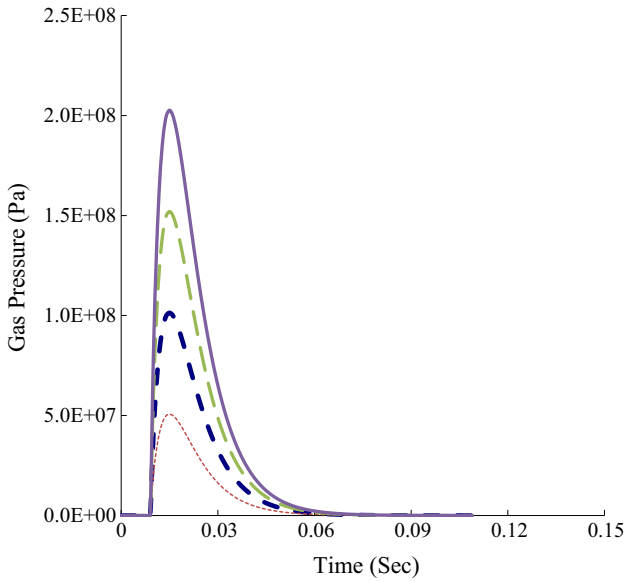

Fig. 8 Blasted gas pressure. Peak pressure ranges from 50 to 200 MPa

lengths of the cracks are much shorter than those of the gas penetration. Similar trend is obtained from the case of linear pressure distribution inside crack (Fig. 5).

The normalized gas pressure inside blasthole in Figs. 4 and 5 decreases as the crack propagates since the total mass of the gas is constant during the crack propagation. Also, the gas pressure in Case 1 is generally bigger than that of the Case 2 because larger gas containment with larger deformation in Case 2 can make gas pressure lower.

Figures 6 and 7 show the comparison of the normalized SIFs and gas pressure variations between $N = 4$ and $N = 8$ for uniform and linear pressure distribution inside crack. In these results, the lengths of the crack with same pressure condition are similar. In other words, initially created cracks due to stress wave do not affect the length of the cracks because of the mechanical interaction between cracks. During the crack propagation, interaction between cracks in case of $N = 8$ is more significant than in case of $N = 4$. Crack opening by internal gas pressure is constrained by adjacent cracks so that gas pressure in case of $N = 8$ is a bit higher than in case of $N = 4$ (Figs. 6, 7). In Table 2, generated crack lengths are summarized with respect to the pressure type.

4 Verification of Analytical Solution

4.1 Numerical Simulation on Crack Propagation Due to Pressure Inside Blasthole

Discrete element method (DEM) has been adopted to simulate the crack propagation in rock and rock mass (Ruest et al. 2006). Discrete fracture network and geological structure can be effectively handled by the DEM. Lisjak and Grasselli (2014) comprehensively summarized the simulation of fracture process in discrete rock masses. Wang and Konietzky (2009) used UDEC (Itasca 2013) to simulate the fractures in jointed rock mass due to blasting-induced stress wave. Particularly, it is found that the Voronoi joint generator is very conducive for numerical simulation of crack creation and propagation due to blasting-induced stress wave.

In this study, UDEC, two-dimensional discrete element method, is implemented to simulate the crack propagation due to blasted gas pressure induced by blasting and to validate the analytical solution presented in previous chapter. Particularly, material properties for numerical model are determined from the reference case. Furthermore, the crack length obtained from numerical analysis is compared with the analytical solution depending on the various blasthole pressure level and ground type to validate the analytical solution.

4.2 Blasting-Induced Gas Pressure

Maximum blasthole pressure (P_B) can be obtained from equation suggested by Morhard (1987), Clark (1987), and Nie and Olsson (2000).

$$P_B = \rho\left(\frac{\mathrm{VOD}^2}{8}\right)\cdot\left(r_c^{2\gamma}\right) \tag{26}$$

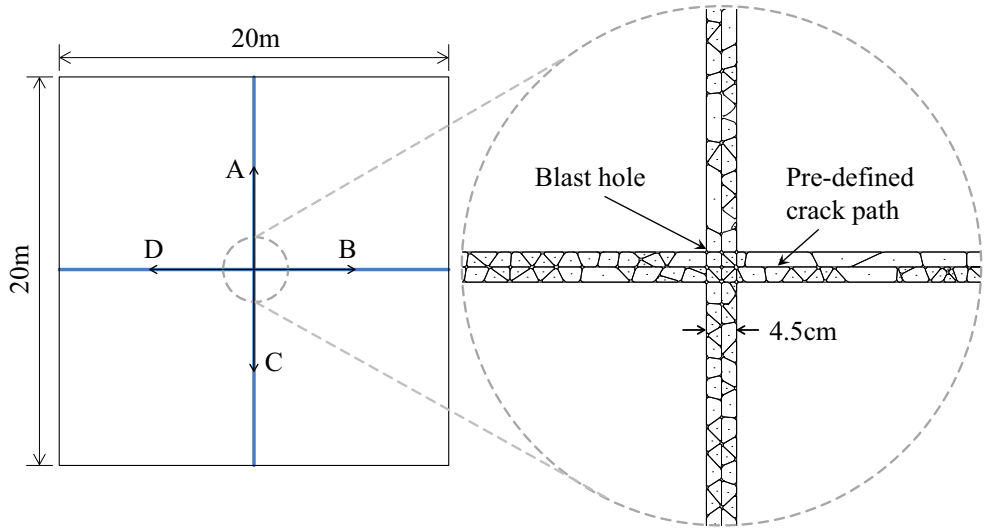

Fig. 9 DEM computation model for simulation of blasting

Table 3 Rock joint properties used for numerical analyses

Properties	Values	
	Case 1	Case 2
Joint shear stiffness (GPa/m)	85	85
Joint normal stiffness (GPa/m)	170	170
Joint friction angle (°)	40	35
Joint cohesion (Pa)	1,009,553	650,974
Joint tension (Pa)	1.0e6	1.0e6
Joint dilation (°)	35	30

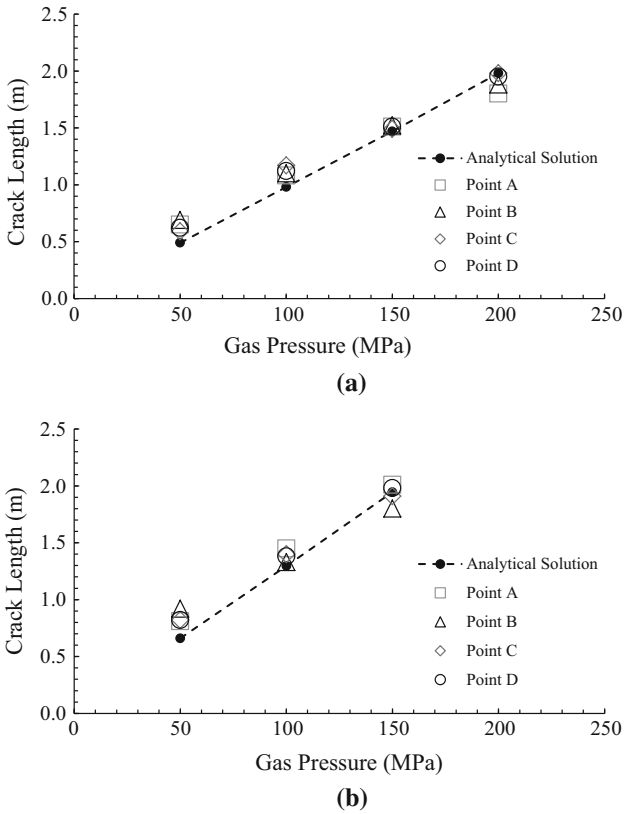

Fig. 10 Comparison of crack length between numerical analysis and analytical solution **a** Case 1 **b** Case 2

where ρ is density of explosive (kg/m^3), VOD is velocity of detonation (m/s), r_c is the decoupling ratio (i.e., = explosive diameter/blasthole diameter), and γ is an adiabatic exponent. Gurit of 17 mm in diameter which is used for precise blasting for contour holes has 2000–3000 m/s of VOD, 1050 kg/m^3 of density. A kimulux42 of 22 mm in diameter which is used for the stopping holes has 3000–4000 m/s of VOD and 1150 kg/m^3 of density (Saharan and Mitri 2008; Song et al. 2014). Thus, the pressure inside blasthole can vary depending on the adiabatic exponent and decoupling ratio. In this study, maximum blasting pressure acting in the blasthole for crack growth ranges from 50 to 200 MPa.

Numerically, blasthole pressure profiles due to blasting can be approximated with John–Wilkinson–Lee (JWL) method (Liu 1997), pressure decay functions (Cho et al. 2003; Lima et al. 2002; Kutter 1967) and direct input of pressure–time profile (Donze et al. 1997; Valliapan et al. 1983) and so on. Although the JWL method can consider the rock-explosive interaction, it is difficult to derive reliable parameters (Liu 1997). The blasthole pressure can be expressed in the form of decay functions (Duvall 1953; Jung et al. 2001; Lima et al. 2002; Olatidoye et al. 1998; Robertson et al. 1994). Gaussian function and triangular

function have been implemented to simplify the blasting pressure. However, the Gaussian function is mainly introduced to avoid numerical errors. In this study, the dynamic pressure $P(t)$ acting on the blasthole is expressed as a transient time history function as follows (Starfield and Pugliese 1968; Histake et al. 1983):

$$P(t) = 4P_{\mathrm{B}}\left[\exp\left(\frac{-16338 \cdot t}{\sqrt{2}}\right) - \exp\left(-\sqrt{2} \cdot 16338 \cdot t\right)\right] \tag{27}$$

where t is the elapsed time. Figure 8 shows the transient time history of blasthole pressure applied to the numerical model. Internal pore pressure is applied in the blasthole according to transient time history function so that the pressure can penetrate and open the crack. To get a clear response, the blasthole pressure is activated after 0.01 s for the model; it is activated at the beginning of the simulation (i.e., 0 s) for the dynamic analysis.

4.3 Numerical Model

The fracturing procedure due to blasting can be divided into two phases; rapid rising detonation pressure initiates multiple cracks around the blasthole and the gas penetration into the crack which leads to crack extension (Majid et al. 2015). Basically, continuing penetration of the explosion gases is guided by initiated crack tips. Cho et al. (2004a, b), Cho and Kaneko (2004), Zhu et al. (2004, 2007a, b, and Ma and An (2008) proposed various random crack generation techniques in rock mass under blasting pressure. Particularly, growth of crack length is mainly contributed by gas pressure. In this study, to validate the analytical solution to estimate the crack length due to blasting, it is assumed that the detonation-induced stress wave creates the crack around the blasthole and gas pressure is responsible for the crack propagation.

Material properties of hard rock and weathered rock used in numerical model are identical to the analytical model. In this study, rock media are assumed as elastic solid as it is assumed in analytical model. Fracture toughness (K_{IC}) is important parameter to be defined to control the crack propagation. In UDEC, residual Coulomb slip with residual strength is used. Sensitivity analysis is carried out to find the optimum joint property for fracture toughness. Cohesion and contact tensile strength are the most significant factors related to toughness. Cohesion and tensile strength of joint are found from trial and error (Kazerani 2011).

Blasted gas pressure has been changed from 50 to 200 MPa for weathered rock and hard rock mass. Transient time history gas pressure is applied in the blasthole as a non-wet pore pressure. 20 m by 20 m rock media with zero velocity at boundary is make it possible to simulate the infinite boundary. As it is reported by Wang and Konietzky (2009), Voronoi tessellation is very useful for simulation of crack propagation. Thus, Voronoi tessellation generator is used to create randomly sized polygonal blocks along the crack paths as it is shown in Fig. 9. Joint area model with Coulomb slip failure is used for joint and joint properties are tabulated in Table 3. When joint shear or tensile strength is exceeded, fracture can be generated along the pre-defined four crack paths.

4.4 Comparisons

Crack lengths in case of uniform pressure inside cracks are measured at four directions (A, B, C and D) as it is presented in Fig. 9, respectively. Due to the random Voronoi tessellation process, the length of crack is slightly different depending on the direction. Crack lengths are obtained from analytical solution depending on the gas pressure and rock condition, and plotted as a dotted line in Fig. 10. And crack length obtained from numerical analysis is plotted as symbols with respect to direction. Figure 10a presents the crack length depending on the gas pressure for Case 1. Crack length increases linearly depending on the pressure. Although the crack length is slightly varied with respect to directions, the crack lengths obtained from numerical analysis show good agreement with analytical solution.

For Case 2 shown in Fig. 10b, crack length obtained from analytical solution increases linearly according to pressure inside blasthole. Definitely, crack length obtained from Case 2 is greater than that obtained from Case 1 both numerical analysis and analytical solution. Analytical solution does not converge when the pressure exceed 150 MPa due to the numerical instability. Within the range of gas pressure (i.e., 50–150 MPa), crack length obtained from analytical solution is very close to numerical result. It implies that the analytical solution can predict the crack length induced by blasting.

Although the analytical solution is derived from simplified assumptions, the crack length obtained from analytical solution is very close to the crack length obtained from dynamic numerical analysis regardless gas pressure and ground condition. Moreover, when the gas penetrates into the crack, this simplified analytical solution can be used to estimate the fragmented zone around the blasthole. In summary, the accuracy of analytical solution is properly validated with the numerical analysis in this study.

5 Conclusions

This paper presents the simple method to predict the fragmentation zone induced by gas pressure during blasting in rock. The fragmentation zone is characterized by analyzing crack propagation from the blasthole. To do this, a model of the blasthole with four ($N = 4$) and eight radial cracks ($N = 8$) of equal length in an infinite elastic plane is considered. In this model, the crack propagation is simulated by using two conditions only, the crack propagation criterion and the mass conservation of the gas.

Generally, the SIF of the crack decreases as crack propagates from the blasthole so that the finally propagated crack length can be determined. As expected, fragmentation zone in weathered rock is wider than that in hard rock because the length of crack obtained in weathered rock is longer than that in hard rock. In addition, gas penetration into the cracks significantly affects the extension of fragmentation zone in rock so that this factor is closely related to the blasting efficiency.

Gas pressure inside blasthole also continues to decrease during crack propagation since the total mass of the gas is assumed to be constant. As crack propagates, deformed blasthole and cracks are repeatedly filled with gas resulting in pressure decrease. In addition, the gas pressure in weathered rock is generally less than that of the hard rock since the crack opening that can contain gas in the weathered rock is much more than in the hard rock. The gas pressure in case of no gas penetration into the cracks is larger than that in case of the gas penetration.

The number of cracks around blasthole has a little effect on the fragmentation formation because of the mechanical interaction between cracks. The mechanical interaction between cracks during crack propagation hinders their openings by internal gas pressure.

Acknowledgements This research was supported by a Grant (15SCIP-B105148-01) from the Construction Technology Research Program funded by the Ministry of Land, Infrastructure, and Transport of the Korean government.

Appendix: Determination of Dimensionless Functions

To determine dimensionless functions, $k_{\mathrm{IZ}}^{\mathrm{crack}}(l, r)$, $f_{\mathrm{Z}}^{\mathrm{crack}}(v, l, r)$, and $f_{\mathrm{Z}}^{\mathrm{blasthole}}(v, l, r)$ in Eqs. (8)–(10), finite element code, FRANC2D (Fracture Analysis Code, Wawrzynek and Ingraffea 1987) is used. Figure 11a shows the typical mesh for the determination of dimensionless functions. The applied mesh is a squared size of 20 m. The blasthole with a radius of $r = 0.045$ m is located in the center of square region within the finer mesh. Figure 11b shows an example of magnified blasthole area with crack length of $l = 0.6$ m. Tables 4, 5, 6 and 7 show the results of calculated dimensionless functions under plane strain conditions.

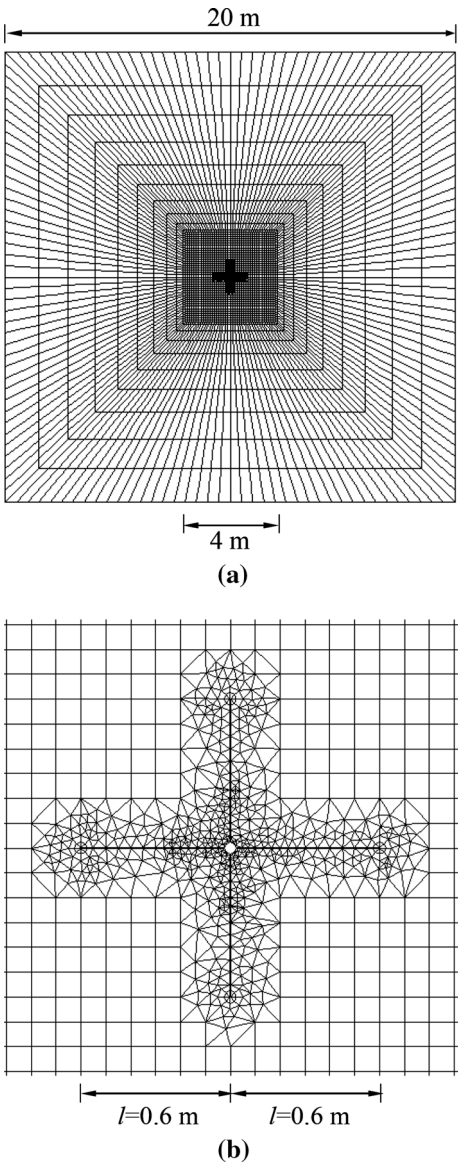

Fig. 11 Example of FRANC2D mesh for the determination of dimensionless functions. **a** FRANC2D mesh and **b** magnified mesh of the blasthole area with crack

Table 4 Dimensionless functions for crack propagation from blasthole in Case 1 ($N = 4$)

Case 1 ($N = 4$)									
l (m)	Problem A			Problem B (uniform pressure)			Problem B (linear pressure)		
	f_A^{crack}	$f_A^{blasthole}$	k_{IA}^{crack}	f_B^{crack}	$f_B^{blasthole}$	k_{IB}^{crack}	f_B^{crack}	$f_B^{blasthole}$	k_{IB}^{crack}
0.0	0.0000	73.4926	0.0000	0.0000	0.0000	0.0000	0.0000	0.0000	0.0000
0.1	25.8185	81.6689	0.2305	105.3423	93.5625	1.6437	58.5168	82.6059	0.4899
0.2	67.1269	86.1910	0.1637	550.4604	147.3893	2.4636	304.0411	114.4749	0.7672
0.3	110.2377	88.8764	0.1339	1348.7320	214.3418	3.0579	745.3741	152.7035	0.9738
0.4	154.1425	90.8033	0.1160	2503.8334	294.0562	3.5845	1384.7359	196.7797	1.1406
0.6	243.0856	93.5579	0.0951	5884.5113	491.8153	4.4183	3257.7512	302.1614	1.4289
0.8	333.0469	95.5416	0.0827	10,701.2581	740.8975	5.1245	5928.3927	430.4028	1.6718
1.0	423.8310	97.1022	0.0743	16,965.9391	1042.3403	5.7534	9404.0157	581.8204	1.8882
1.2	515.3686	98.3949	0.0682	24,693.1856	1397.1968	6.3242	13,692.0162	756.8169	2.0853
1.4	607.7327	99.5044	0.0634	33,901.8180	1807.2820	6.8478	18,803.5101	956.0376	2.2670
1.6	700.9646	100.4797	0.0597	44,610.9054	2273.8800	7.3461	24,749.1019	1180.0244	2.4407

Table 5 Dimensionless functions for crack propagation from blasthole in Case 2 ($N = 4$)

Case 2 ($N = 4$)									
l (m)	Problem A			Problem B (uniform pressure)			Problem B (linear pressure)		
	f_A^{crack}	$f_A^{blasthole}$	k_{IA}^{crack}	f_B^{crack}	$f_B^{blasthole}$	k_{IB}^{crack}	f_B^{crack}	$f_B^{blasthole}$	k_{IB}^{crack}
0.0	0.0000	15.2697	0.0000	0.0000	0.0000	0.0000	0.0000	0.0000	0.0000
0.1	24.7857	27.3767	0.2305	101.1286	47.9828	1.6437	56.1735	26.9959	0.4899
0.2	64.4418	35.3439	0.1637	528.4420	201.7448	2.4636	291.8794	98.3823	0.7672
0.3	105.8282	40.4463	0.1339	1294.7827	468.8772	3.0579	715.5591	219.5194	0.9738
0.4	147.9768	44.2893	0.1160	2403.6801	853.0238	3.5845	1329.3465	391.8171	1.1406
0.6	233.3622	49.9760	0.0951	5649.1308	1981.1280	4.4183	3127.4412	893.9925	1.4289
0.8	319.7250	54.2308	0.0827	10,273.2077	3597.1633	5.1245	5691.2570	1610.2907	1.6718
1.0	406.8778	57.6697	0.0743	16,287.3015	5712.6482	5.7534	9027.8551	2545.5930	1.8882
1.2	494.7539	60.5778	0.0682	23,705.4582	8338.4395	6.3242	13,144.3355	3704.5257	2.0853
1.4	583.4234	63.1164	0.0634	32,545.7453	11,491.0431	6.8478	18,051.3697	5093.1411	2.2670
1.6	672.9260	65.3798	0.0597	42,826.4692	15,183.1821	7.3461	23,759.1378	6716.8168	2.4407

Table 6 Dimensionless functions for crack propagation from blasthole in Case 1 ($N = 8$)

Case 1 ($N = 8$)									
l (m)	Problem A			Problem B (uniform pressure)			Problem B (linear pressure)		
	f_A^{crack}	$f_A^{blasthole}$	k_{IA}^{crack}	f_B^{crack}	$f_B^{blasthole}$	k_{IB}^{crack}	f_B^{crack}	$f_B^{blasthole}$	k_{IB}^{crack}
0.0	0.0000	73.4926	0.0000	0.0000	0.0000	0.0000	0.0000	0.0000	0.0000
0.1	14.4605	81.9440	0.1704	63.4038	97.3108	1.3066	33.5804	83.9708	0.3374
0.2	37.0526	86.3624	0.1193	325.9539	160.4288	1.9321	171.8133	119.0508	0.5282
0.3	60.4850	89.0561	0.0962	794.1409	243.3179	2.3668	419.1817	162.7645	0.6643
0.4	84.3673	91.0016	0.0841	1469.9344	346.1803	2.7893	777.2447	214.9697	0.7856
0.6	132.7614	93.7929	0.0685	3449.3957	611.9919	3.4196	1825.8084	344.6642	0.9814
0.8	181.8000	95.8186	0.0597	6273.1672	959.7933	3.9685	3322.4751	508.6167	1.1522
1.0	231.2931	97.4336	0.0537	9944.1303	1393.9826	4.4553	5270.9664	708.2915	1.3045
1.2	281.4824	98.7866	0.0493	14,493.0834	1918.2556	4.9021	7684.9123	945.0855	1.4448
1.4	332.7329	99.9525	0.0460	19,974.5101	2535.0823	5.3167	10,586.9957	1219.9367	1.5761
1.6	384.1799	100.9927	0.0433	26,318.0150	3250.8020	5.7082	13,956.7149	1535.0707	1.7005

Table 7 Dimensionless functions for crack propagation from blasthole in Case 2 ($N = 8$)

Case 2 ($N = 8$)									
l (m)	Problem A			Problem B (uniform pressure)			Problem B (linear pressure)		
	f_A^{crack}	$f_A^{blasthole}$	f_B^{crack}	$f_B^{blasthole}$	k_{IB}^{crack}	k_{IB}^{crack}	f_B^{crack}	$f_B^{blasthole}$	k_{IB}^{crack}
0.0	0.0000	15.2697	0.0000	0.0000	0.0000	0.0000	0.0000	0.0000	0.0000
0.1	13.8821	30.0910	0.1704	60.8677	68.0824	1.3066	32.2372	35.5501	0.3374
0.2	35.5705	39.3179	0.1193	312.9158	298.4165	1.9321	164.9408	135.4115	0.5282
0.3	58.0656	45.4126	0.0962	762.3753	707.9168	2.3668	402.4144	308.6715	0.6643
0.4	80.9926	50.0253	0.0841	1411.1370	1303.6294	2.7893	746.1549	558.6235	0.7856
0.6	127.4510	56.9381	0.0685	3311.4199	3065.8077	3.4196	1752.7761	1294.4744	0.9814
0.8	174.5280	62.1618	0.0597	6022.2405	5609.8062	3.9685	3189.5761	2353.6271	1.1522
1.0	222.0414	66.4390	0.0537	9546.3651	8974.1201	4.4553	5060.1278	3749.5609	1.3045
1.2	270.2231	70.1013	0.0493	13,913.3600	13,196.5456	4.9021	7377.5158	5496.5191	1.4448
1.4	319.4236	73.3203	0.0460	19,175.5297	18,306.1081	5.3167	10,163.5159	7605.6864	1.5761
1.6	368.8127	76.2278	0.0433	25,265.2944	24,354.2675	5.7082	13,398.4463	10,095.0783	1.7005

References

Ali F, Mark L (2014) DEM-SPH simulation of rock blasting. Comput Geotech 55:158–164

Brinkman JR (1987) Separating shock waves and gas expansion breakage mechanisms. In: Proceedings of the 2nd international symposium on rock fragmentation by blasting. Keystone, pp 6–15

Chen SG, Zhao J (1998) A study of UDEC modelling for blast wave propagation in jointed rock masses. Int J Rock Mech Min Sci 35:93–99

Cho SH, Kaneko K (2004) Influence of the applied pressure waveform on the dynamic fracture processes in rock. Int J Rock Mech Min Sci 41:771–784

Cho SH, Risei K, Kato M (2002) Development of numerical simulation method for dynamic fracture propagation due to gas pressurization and stress wave. In: Proceedings of 2002 ISRM regional symposium (3rd Korea-Japan joint symposium) on rock engineering problem and approaches in underground construction, Seoul, July 22–24, pp 755–762

Cho SH, Miyake H, Kimura T, Kaneko K (2003) Effect of the waveform of applied pressure on rock fracture process in one free-face. J Sci Technol Energ Mater 64(3):116–125

Cho SH, Ogata Y, Kaneko K (2004a) Strain-rate dependency of the dynamic tensile strength of rock. Int J Min Sci Technol 40:763–777

Cho SH, Nakamura Y, Kaneko K (2004b) Dynamic fracture process analysis of rock subjected to stress wave and gas pressurization. Int J Min Sci Technol 41:433–440

Clark GB (1987) Principles of rock fragmentation. Wiley, London, p 610

Donze FV, Bouchez J, Magnier SA (1997) Modeling fractures in rock blasting. Int J Rock Mech Min Sci 34(8):1153–1163

Duvall WI (1953) Strain wave shapes in rock near explosions. Geophysics 18(2):310–323

Fjellborg S, Olsson M (1996) Long drift rounds with large cut holes at LKAB. SveBeFo Report No. 27, Swedish Rock Engineering Research, Stockholm

Garnsworthy RK (1990) The mathematical modeling of rock fragmentation by high pressure arc discharges. In: 3rd international symposium on rock fragmentation by blasting, Brisbane, pp 143–147

Gholami A, Rahman SS, Natarajan S (2013) Simulation of hydraulic fracture propagation using XFEM. In: EAGE symposium, sustainable earth sciences. Pau, Sept 30–Oct 4

Goodarzi M, Mohammadi S, Jafari A (2011) Analysis of gas-driven crack propagation around a blast hole with the extended finite element method. In: Proceedings of the 2nd international symposium on computational geometry (COMGEO II), April 27–29, pp 425–433

Goodarzi M, Salmi EF, Mohammadi S (2013) Numerical modeling of gas fracturing with the extended finite element method. In: Proceedings of the end international symposium on computational geometry (COMGEO III), Aug 21–23, pp 706–716

Gordeliy E, Peirce A (2013) Coupling schemes for modeling hydraulic fracture propagation using the XFEM. Comput Methods Appl Mech Eng 253:305–322

Histake M, Sakurai S, Ito T, Kobayashi Y (1983) Analytical contribution to tunnel behavior caused by blasting. In: Proceedings of 5th International congress on rock mechanics, Melbourne, pp E191–E194

Hustrulid W (2010) Some comments regarding development drifting practices with special emphasis on caving applications. In: Potvin AGG (ed) Proceedings of the Caving 2010 symposium on Block and Sublevel Caving, Perth Australia, pp 3–44

Itasca Consulting Group, Inc. (2013) UDEC-Universal Distinct Element Code. Version 5.0. User Manual

Jung WJ, Utagava M, Ogata Y, Seto M, Katsuyama K, Miyake A, Ogava T (2001) Effects of rock pressure on crack generation during tunnel blasting. J Jpn Explos Soc 62(3):138–146

Kanchibolta SS, Valery W, Morrell S (1999) Modeling fines in blast fragmentation and its impact on crushing and grinding. In: Proceedings of Explo '99-A Conference on Rock Breaking. The Australasian Institute of Mining and Metallurgy, Brisbane, pp 137–144

Kazerani T (2011) Micromechanical study of rock fracture and fragmentation under dynamic loads using discrete element method. Doctoral dissertation, ÉCOLE POLYTECHNIQUE FÉDÉRALE DE LAUSANNE

Kutter HK (1967) The interaction between stress wave and gas pressure in the fracture process of an underground explosion in rock, with particular application to presplitting (Unpublished). Ph.D. Thesis. University of Minnesota, Minneapolis, p 234

Lima ADR, Romanel C, Roehl DM, Araujo TD (2002) An adaptive strategy for the dynamic analysis of rock fracturing by blasting. In: Proceedings of the international conference computational engineering and science (ICES'02), Reno

Lisjak A, Grasselli G (2014) A review of discrete modeling techniques for fracturing processes in discontinuous rock masses. J Rock Mech Geotech Eng 6(4):301–314

Liu L (1997) Continuum modelling of rock fragmentation by blasting (Unpublished). Ph.D. thesis. Queen's University, p 240

Ma GW, An XM (2008) Numerical simulation of blasting-induced rock fractures. Int J Rock Mech Min Sci 45:966–975

Ma GW, Hao H, Zhou YX (1998) Modeling of wave propagation induced by underground explosion. Comput Geotech 22:283–303

Maji AK, Wang JL (1992) Experimental study of fracture processes in rock. Rock Mech Rock Eng 25:25–47

Majid G, Soheil M, Ahmad J (2015) Numerical analysis of rock fracturing by gas pressure using the extended finite element method. Pet Sci 12:304–315

Minchinton A, Lynch P (1996) Fragmentation and heave modeling using a coupled discrete element gas code. In: Mohanty B (ed) Rock fragmentation by blasting. A.A. Balkema, Rotterdam, pp 71–80

Mindess S (1991) Fracture process zone detection. RILEM Committee 89-FMT Report, fracture mechanics of concrete: test methods, RILEM, pp 231–262

Mohammadnejad T, Khoei AR (2013) An extended finite element method for hydraulic fracture propagation in deformable porous media with the cohesive crack model. Finite Elem Anal Des 73:77–95

Morhard RC (1987) Explosives and rock blasting. Atlas Powder Company, Washington

Nie S, Olsson M (2000) Study of fracture mechanism by measuring pressure history in blast holes and crack lengths in rock. In: Proceedings of the 27th annual conference explosives and blasting technique, Orlando, pp 291–300

Nilson RH, Proffer WJ, Duff RE (1985) Modelling of gas-driven fractures induced by propellant combustion within a borehole. Int J Rock Mech Min Sci Geomech Abstr 22(1):3–19

Olatidoye O, Sarathy S, Jones G, McIntyre C, Milligan L (1998) A representative survey of blast loading models and damage assessment methods for buildings subject to explosive blasts. Report by Nichols Research Corporation. Report No. CEWES MSRC = PET TR = 98-36, p 14

Olsson M, Bengt N, Lasse W, Andersson C, Christiansson R (2004) Äspö HRL: experiences of blasting of the TASQ tunnel. R-04-73, SKB, Stockholm, Sweden. In: Langefors U, Kihlström B (eds) The modern technique of rock blasting. Wiley, Stockholm, 1963

Onederra IA, Furtney JK, Sellers E, Iverson S (2013) Modeling blast induced damage from a fully coupled explosive charge. Int J Rock Mech Min Sci 58:73–84

Ouchterlony F (1974) Fracture mechanics applied to rock blasting, advances in rock mech. In: Proceedings of the 3rd ISRM Congress. 11-B, Denver, pp 1377–1383

Ouchterlony F (1997) Prediction of crack lengths in rock after cautious blasting with zero inter-hole delay. Int J Blast Fragm 1:417–444

Ouchterlony F, Olsson M, Bergqvist I (2002) Towards new Swedish recommendations for cautious perimeter blasting. Fragblast 6(2):235–261

Paine AS, Please CP (1994) An improved model of fracture propagation by gas during rock blasting-some analytical results. Int J Rock Mech Min Sci Geomech Abstr 31(6):699–706

Persson PA, Holmberg R, Lee J (1994) Rock blasting and explosive engineering. CRC Press, Boca Raton, London, New York, Washington DC

Potyondy D, Cundall P, Sarracino R (2004) Modeling of shock- and gas-driven fractures induced by a blast using bonded assemblies of spherical particles. In: Mohanty B (ed) Rock fragmentation by blasting. A.A. Balkema, Rotterdam (1996), pp 55–62

Ren QW, Dong YW, Yu TT (2009) Numerical modeling of concrete hydraulic fracturing with extended finite element method. Sci China Ser E 52(3):559–565

Robertson NJ, Hayhurst CJ, Fairlie GE (1994) Numerical simulation of explosion phenomena. Int J Comput Appl Technol 7(3–6):316–329

Rossmanith HP (ed) (1983) Rock fracture mechanics. Springer, Wien, New York, pp 69–150

Ruest M, Cundall P, Guest A, et al. (2006) Developments using the particle flow code to simulate rock fragmentation by condensed phase explosives. In: Proceedings of the 8th international symposium rock fragmentation by blasting—FRAGBLAST-8, Santiago, May 8–11, pp 140–151

Saharan MR, Mitri HS (2008) Numerical procedure for dynamic simulation of discrete fractures due to blasting. Rock Mech Rock Eng 41(5):641–670

Song KI, Oh TM, Cho GC (2014) Abrasive waterjet aided vibration reduced tunnel blasting technique-numerical analysis. KSCE J Civ Eng 18(4):1165–1175

Starfield AM, Pugliese JM (1968) Compression waves generated in rock by cylindrical explosive charges: a comparison between a computer model and field measurements. Int J Rock Mech Min Sci Geom Abst 5(1):65–77

Torbica S, Lapcevic V (2015) Estimating extent and properties of blast-damaged zone around underground excavations. Rem Rev Esc Minas 68(4):441–453

Valliapan S, Lee IK, Murti V, Ang KK, Ross AH (1983) Numerical modelling of rock fragmentation. In: Proceedings of the 1st International symposium rock fragmentation by blasting—FRAGBLAST 1. Balkema, Rotterdam, pp 375–390

Wang ZL, Konietzky H (2009) Modelling of blast-induced fractures in jointed rock mass. Eng Fract Mech 76:1945–1955

Wang Z, Yong-chi L, Wang J (2008) Numerical analysis of blast-induced wave propagation and spalling damage in a rock plate. Int J Rock Mech Min Sci 45:600–608

Wawrzynek PA, Ingraffea AR (1987) Interactive finite element analysis of fracture processing: an integrated approach. Theor Appl Fract Mech 8:137–150

Wei X, Zhao Z, Gu J (2009) Numerical simulations of rock mass damage induced by underground explosion. Int J Rock Mech Min Sci 46:1206–1213

Whittaker BN, Singh RN, Sun G (1992) Rock fracture mechanics: principles, design and applications. In: Development in Geotechnical Engineering, vol 71. Elsevier, Amsterdam, London, New York, Tokyo, pp 443–480

Zhu WC, Tang CA, Huang ZP et al (2004) A numerical study of the effect of loading conditions on the dynamic failure of rock. Int J Rock Mech Min Sci 41(3):424

Zhu ZM, Mohanty B, Xie HP (2007a) Numerical investigation of blasting-induced crack initiation and propagation in rocks. Int J Rock Mech Min Sci 44:412–424

Zhu Z, Mohanty B, Xie H (2007b) Numerical investigation of blasting-induced crack initiation and propagation in rocks. Int J Rock Mech Min Sci 44:412–424